

# Three-dimensional nanofabrication using HSQ/PMMA bilayer resists

Running title: Three-dimensional nanofabrication

Running authors: Do et al.

Hyung Wan Do<sup>a), d)</sup>, Jae-Byum Chang<sup>b)</sup>, Karl K. Berggren<sup>a), c)</sup>

<sup>a)</sup> Department of Electrical Engineering and Computer Science, Massachusetts Institute of Technology, Cambridge, Massachusetts 02139

<sup>b)</sup> Department of Materials Science and Engineering, Massachusetts Institute of Technology, Cambridge, Massachusetts 02139

<sup>c)</sup> American Vacuum Society member

<sup>d)</sup> Electronic mail: [hwdo@mit.edu](mailto:hwdo@mit.edu)

In this work, the authors developed two processes for fabricating three-dimensional (3D) nanostructures using a hydrogen silsesquioxane (HSQ) and poly(methylmethacrylate) (PMMA) bilayer resist stack. The resist stack was patterned in a single electron-beam writing step without removing the wafer. The resulting 3D nanostructures naturally achieved vertical self-alignment without the need for any intermediate alignment. Self-aligned mushroom-shaped posts and freestanding supported structures were demonstrated.

# I. INTRODUCTION

Three-dimensional (3D) devices are difficult to fabricate, but offer unique advantages over planar devices for many applications. There has been a growing interest in 3D devices such as photonic crystals and metamaterials,<sup>1,2</sup> and nanoelectromechanical systems (NEMS).<sup>3</sup> However, methods for generating 3D devices are generally slow and expensive. Therefore, a simple and rapid fabrication process for complex 3D nanostructures is necessary. Methods for fabricating such 3D nanostructures using electron-beam lithography (EBL) include consecutive overlay exposures<sup>4,5</sup> or low- and high-electron energy exposures.<sup>6,7,8</sup> However, these approaches require alignment markers and accurate alignment routines for each additional layer. 3D nanostructures have also been fabricated using grayscale lithography,<sup>9</sup> but in this approach, the feature size was limited to several hundred nanometers.

A common approach used to circumvent the problem of 3D nanostructure fabrication is to use a bilayer resist stack.<sup>10,11,12</sup> Using a hydrogen silsesquioxane (HSQ) and poly(methylmethacrylate) (PMMA) bilayer resist stack, 3D nanostructures have been fabricated by patterning the top HSQ layer and reactive-ion etching of the bottom PMMA layer.<sup>10,11</sup> PMMA and poly(methylglutarimide) (PMGI) bilayer have also been used to pattern controlled 3D undercut structures.<sup>12</sup> However, these methods had restrictions on the final structures because all structures must be derived from only undercut structures.

Here, we describe self-aligned methods of fabricating 3D nanostructures using EBL of HSQ and PMMA, which allows more arbitrary patterns. HSQ is an inorganic, negative-tone, ultra-high resolution resist capable of resolving sub-10-nm half-pitch structures.<sup>13,14</sup> PMMA is an organic positive-tone resist that can also operate in negative-

tone with ultra-high resolution when exposed to a dose about 30 times higher than the positive dose.<sup>15</sup> In this work, we demonstrate two processes where the difference in dose sensitivity between HSQ and PMMA was used to produce self-aligned 3D nanostructures. Mushroom-shaped posts and freestanding supported structures were created without requiring feature alignment between layers. Figure 1 shows an example of a 3D nanostructure that was fabricated with our approach.

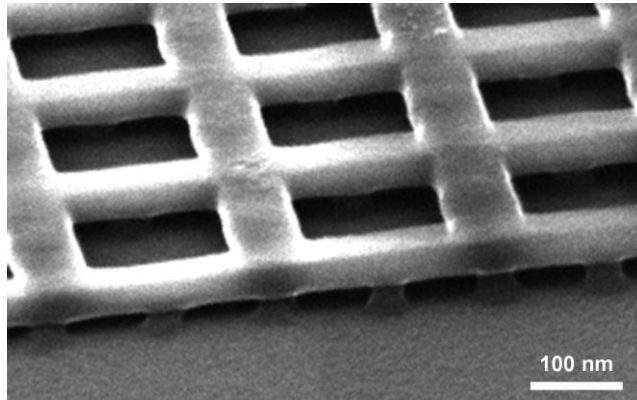


Figure 1. SEM image of a 3D supported cross grid structure from sample III fabricated by using the methods described in this paper (tilt angle of  $55^\circ$ ). Freestanding top layer was patterned in HSQ and supporting bottom layer was patterned in PMMA. The two layers were exposed in a single electron-beam writing step without intermediate alignment of the pattern.

## II. EXPERIMENTAL

The key to realizing self-aligned 3D nanostructures on surfaces lies in designing an appropriate resist stack and electron-beam-exposure process. The process details were optimized to realize complex and well-supported 3D nanostructures with adequate dimensional control and precision. The resulting features were then analyzed by using

secondary electron imaging. We describe here two processes for 3D device fabrication, and the microscopy methods used to analyze the structures.

Figure 2 illustrates the fabrication steps required to create 3D nanostructures using HSQ/PMMA bilayer resists. We developed two processes: (1) figure 2(a) shows the single-dot exposure process; and (2) figure 2(b) shows the double-area exposure process. In both processes, we used the sensitivity difference between HSQ and PMMA to fabricate self-aligned 3D nanostructures.

In the single-dot exposure process, we used a single exposure dose to pattern the bilayer resist stack. The resist stack was prepared by spin coating HSQ and PMMA on a silicon substrate. PMMA was spin coated first and was baked at 200°C for 2 min on a hot plate. HSQ was then spin coated on the PMMA. One sample was coated with 22 nm of PMMA followed by 22 nm of HSQ. A second sample was coated with 37 nm of PMMA followed by 28 nm of HSQ. A third sample was coated with 48 nm of PMMA followed by 39 nm of HSQ. We will refer to these as sample I, sample II, and sample III. The thickness was determined by ellipsometry. A bilayer resist stack was formed without resist intermixing (step 1). A Raith 150 EBL system was used to expose dot arrays with doses ranging from 200 fC/dot ( $\sim 1.2 \times 10^6$  electrons/dot) to 3200 fC/dot ( $\sim 2.0 \times 10^7$  electrons/dot) at 30 kV acceleration voltage and 200 pA beam current. Because HSQ has higher dose sensitivity than negative-tone PMMA, the HSQ was overdosed relative to the PMMA. As a result, larger diameter HSQ disks were formed on top of smaller diameter PMMA posts (step 2). After exposure, the samples were developed in a high-contrast salty developer (1% NaOH and 4% NaCl in de-ionized water)<sup>13</sup> at 24°C for 4 min followed by a de-ionized water rinse for 3 min and blow drying with nitrogen (N<sub>2</sub>) gas to

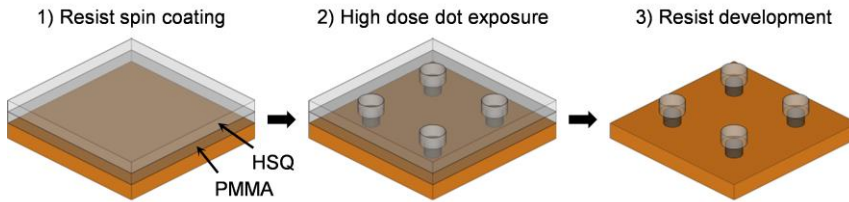
remove unexposed HSQ. To remove lightly exposed PMMA and unexposed PMMA, the samples were sequentially developed in methyl isobutyl ketone (MIBK) at 18°C for 4 min,<sup>15</sup> spray rinsed with isopropanol (IPA) for 1 min, developed in acetone at 18°C for 3 min, and blown dry with N<sub>2</sub> gas (step 3).

To better control the size and shape of the nanostructures on each resist layer, we developed a double-area exposure process in which smaller features on the bottom PMMA layer were defined using high dose exposures, and larger features on the top HSQ layer were defined using low dose exposures. Both layers were exposed in a single writing step without removing the wafer. In the double-area exposure process, the bilayer resist stack was prepared as in the single-dot exposure process (step 1). A Raith 150 EBL system was used to expose arrays of 50-nm-diameter circles with a dose of 24000  $\mu\text{C}/\text{cm}^2$  ( $\sim 1500$  electrons/ $\text{nm}^2$ ). During this step, 65-nm-diameter circular disks were formed in the HSQ layer due to overdose (step 2). In the same writing step, 75 nm  $\times$  2  $\mu\text{m}$  rectangles were exposed over the circles with a dose of 4000  $\mu\text{C}/\text{cm}^2$  ( $\sim 250$  electrons/ $\text{nm}^2$ ). This dose was sufficient to crosslink the HSQ, but was insufficient to severely affect the PMMA. Therefore, the rectangular line structures were only formed in the HSQ layer (step 3). After development, the lightly exposed PMMA under the HSQ line structures were removed and freestanding 3D nanostructures were formed (step 4).

Metrology was performed by examining the 3D nanostructures using a scanning electron microscope (SEM). Top down SEM images were acquired using a Raith 150 scanning electron microscope operated with 10 kV acceleration voltage and 6 mm working distance. Tilted SEM images were obtained using a Zeiss Orion helium ion

microscope and FEI Helios dual beam system. The operating conditions were 35 kV and 10 mm for the helium ion microscope, and 5 kV and 4 mm for the dual beam system.

**(a) Single-dot exposure process**



**(b) Double-area exposure process**

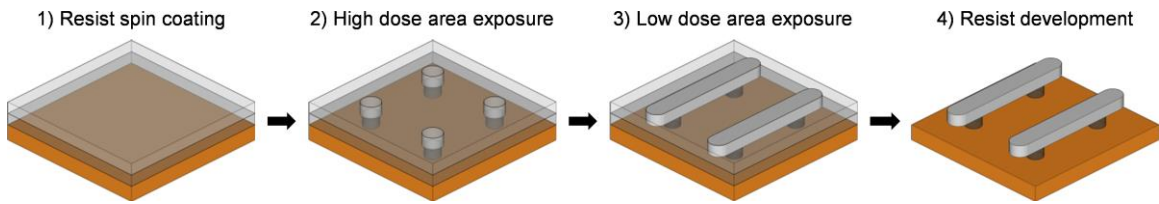


Figure 2. (Color online) Schematic diagram showing process steps for single-dot exposure process and double-area exposure process. (a) HSQ/PMMA bilayer resist stack was prepared with HSQ on top of PMMA. Both resist layers were exposed from above with an electron beam. The HSQ was overdosed relative to the PMMA, resulting in a larger top structure and overhang. The result was mushroom-shaped posts. (b) The same resist stack as in (a) but the exposure was done by using two immediately sequential doses. In the first lithography step, the bottom layer features were exposed using a high dose, while in the second lithography step, the top layer features were exposed at a dose that was too low to affect the initial bottom layer exposure. The result was free standing linear HSQ structures supported by PMMA posts.

### III. RESULTS

By using the methods described in the previous section, we were able to fabricate a range of 3D nanostructures including mushroom-shaped posts, supported lines, and

supported cross grids. Here, we describe those results so that we can draw conclusions about which methods are preferred under different circumstances.

Figure 3 shows the 3D nanostructures fabricated using the single-dot exposure process, demonstrating overhung structures. In figure 3(a),  $200\text{ nm} \times 200\text{ nm}$  pitch dot arrays were exposed at a dose of  $3200\text{ fC/dot}$  ( $\sim 2.0 \times 10^7$  electrons/dot), resulting in  $108\text{-nm}$ -diameter HSQ disks and  $40\text{-nm}$ -diameter PMMA posts. Such mushroom-shaped posts were created due to the sensitivity difference between the two resists. The diameter of both structures was determined by the single-dot exposure dose and the structures thus naturally achieved vertical self-alignment. In figure 3(b),  $200\text{ nm} \times 75\text{ nm}$  pitch dot arrays were exposed at a dose of  $1132\text{ fC/dot}$  ( $\sim 7.1 \times 10^6$  electrons/dot). Because the dots were positioned sufficiently close to each other, neighboring,  $57\text{-nm}$ -diameter HSQ disks merged and formed wavy lines on top of  $28\text{-nm}$ -diameter PMMA posts.

Pattern collapse was observed as shown in figure 3(c) when care was not taken during the development and drying process. Here, the HSQ layer was  $28\text{ nm}$  thick and the PMMA layer was  $37\text{ nm}$  thick. The dot arrays were exposed at a dose of  $566\text{ fC/dot}$  ( $\sim 3.5 \times 10^6$  electrons/dot), resulting in  $40\text{-nm}$ -diameter HSQ disks and  $24\text{-nm}$ -diameter PMMA posts. The collapsed nanostructures clearly showed the two resist materials as indicated in the inset of figure 3(c).

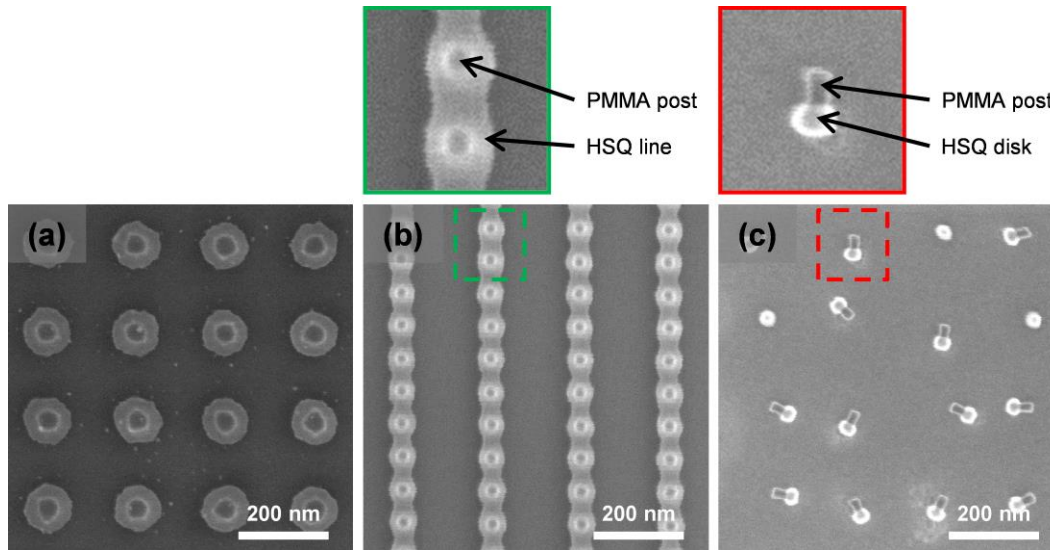


Figure 3. (Color online) SEM images of 3D nanostructures fabricated from the single-dot exposure process. All structures were from sample II. (a) Mushroom-shaped post structures. (b) Closely spaced linear arrays of posts resulted in connected top layer HSQ patterns supported by PMMA posts in the underlayer. (c) Same post structures as in (a) but where 5.65 times less exposure dose was used. The structures collapsed during the development and drying process.

The 3D nanostructures fabricated using the double-area exposure process are shown in figure 4. In figure 4(a), 75-nm-diameter disks were patterned in HSQ using low dose exposures, and 50-nm-diameter posts were patterned in PMMA using high dose exposures. Mushroom-shaped nanostructures similar to those in figures 3(a) and 3(c) could be created with more dimensional precision than could be achieved in the single-dot exposure process. Figure 4(b) shows 60-nm-wide line structures in HSQ supported by 30-nm-diameter PMMA posts. The tilted SEM image demonstrated that the line structures were truly freestanding. Since features on each resist layer could be more accurately controlled using the double-area exposure process, complex 3D nanostructures

could be fabricated as shown in figure 4(c), where a 75-nm-wide cross grid was supported by 50-nm-diameter PMMA posts.

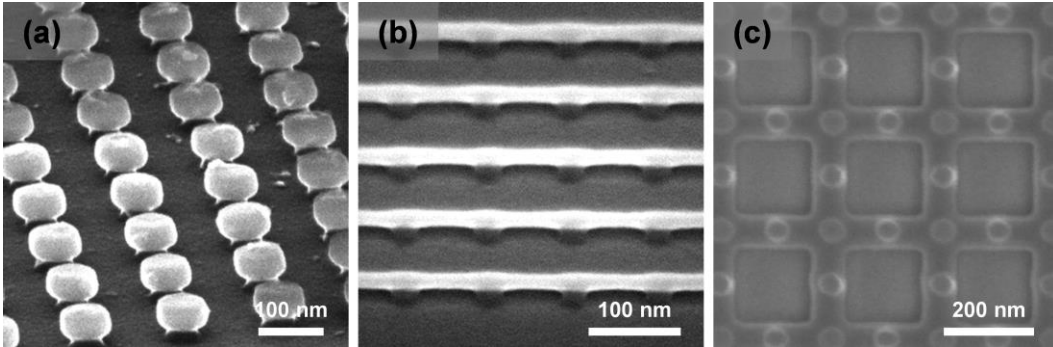


Figure 4. SEM images of 3D nanostructures fabricated from the double-area exposure process. The first structure was from sample III and the other two structures were from sample I. (a) Mushroom-shaped posts with well-defined top disks over lower posts (tilt angle of  $55^\circ$ ). (b) Freestanding linear top layer structures with a lower layer post support (tilt angle of  $45^\circ$ ). (c) Freestanding cross grid structures with a lower layer post support.

## IV. DISCUSSION

A number of non-idealities were encountered and lessons learned as a result of our work. The single-dot exposure process could be thought of as a special case of the double-area exposure process where dot arrays are exposed in the high dose exposure step, and the low dose exposure step is omitted. Therefore, the single-dot exposure process proved more difficult to control than the double-area exposure process, from the perspective of both structure dimensions and edge roughness. Furthermore, overhung structures resulted in pattern collapse in the single-dot exposure process. The causes and remedies for these observations are discussed here.

We were able to better control the size and shape of the nanostructures on each resist layer by using the double-area exposure process than using the single-dot exposure process. Mushroom-shaped posts shown in figures 3(a), 3(c), and 4(a) could be fabricated using both processes. However, it was difficult to independently control the features on each resist layer in the single-dot exposure process because both layers were patterned by a single exposure dose. Therefore, the nanostructures in the top layer and the bottom layer had the same shape with only a difference in size. The possible structures were limited to mushroom-shaped posts (figures 3(a) and 3(c)) and structures formed from merged posts (figure 3(b)). On the other hand, it was possible to precisely control the feature dimensions in the double-area exposure process as long as the size of the low dose exposure was larger than the size of the structures already defined by the high dose exposure, since two separate exposure steps were used to pattern each resist layer. Using two exposure steps gave more freedom in designing the 3D nanostructures. Contrary to figure 3(b), figure 4(b) did not show any waviness in the top layer because the line structures were formed by exposing rectangular patterns rather than by merging neighboring disks. Figure 4(c) demonstrates one possible nanostructure that can only be created with the double-area exposure process, a HSQ cross grid supported by PMMA posts.

In the single-dot exposure process, the top HSQ disks showed significant edge roughness as the dot dose was increased. Figures 3(a) and 3(c) illustrate the difference in the edge roughness where the exposure dose used in 3(a) was 5.65 times the exposure dose used in 3(c). Because the bilayer resist stack was exposed with a dot dose necessary to achieve negative-tone PMMA, the sensitive HSQ layer was significantly overdosed

when a high dose was used to expose both layers. As a result, the areal-dose-density slope at the critical dose for HSQ exposure was significantly lower than it would be for an area dose (where most of the dose comes from the well-defined primary beam, rather than backscattering and beam skirts). This lower dose-density-slope resulted in less well-defined feature edges. This issue was solved by using the double-area exposure process where the size of the structures was controlled by the dimensions of the exposed pattern rather than the dose.

Finally, we developed a simple way to avoid collapse. We observed that pattern collapse occurred during the PMMA development and drying process. Originally in the process, the samples were sonicated in 18°C acetone for 3 min to remove unexposed PMMA. This process was modified by removing the sonication step. In addition, the final structure was rinsed with a low surface tension liquid, IPA prior to drying.<sup>16</sup>

## **V. CONCLUSIONS**

The two processes described in this work are advantageous compared to previous approaches in that the resulting 3D nanostructures are self-aligned and thus avoid the need for any alignment routine. We successfully fabricated various 3D nanostructures such as freestanding cross grid supported by posts. Other types of structures could be benefited from our method. For example, sheets supported by lines or grids could be used as nanochannels for nanofluidic devices. Moreover, we believe that our method can be extended to a multilayer resist stack with different resist combinations as long as the resist layers have different dose sensitivity to electron beam and do not intermix with each other. We also point out that feature sizes might be tuned further by varying the development process from layer to layer. We expect that this simple method for creating

self-aligned 3D nanostructures will have potential applications in plasmonic structures and nanomechanical devices.

## ACKNOWLEDGMENTS

The authors would like to thank James Daley and Mark Mondol for technical assistance, Samuel Nicaise and Dr. Hong Kyoong Choi for help with imaging, and Dr. Richard Hobbs and Vitor Manfrinato for valuable discussions. MIT's Scanning-Electron-Beam Lithography facility at the Research Laboratory of Electronics (SEBL at RLE) was used for this study. This work was supported by Taiwan Semiconductor Manufacturing Company and National Science Foundation under Award Number DMR-1234169.

<sup>1</sup>G. von Freymann, A. Ledermann, M. Thiel, I. Staude, S. Essig, K. Busch, and M. Wegener, *Adv. Funct. Mater.* **20**, 1038 (2010).

<sup>2</sup>C. M. Soukoulis and M. Wegener, *Nat. Photonics* **5**, 523 (2011).

<sup>3</sup>H. G. Craighead, *Science* **290**, 1532 (2000).

<sup>4</sup>J. Vila-Comamala, S. Gorelick, V. A. Guzenko, and C. David, *J. Vac. Sci. Technol. B* **29**, 06F301 (2011).

<sup>5</sup>L. T. Varghese, L. Fan, J. Wang, Y. Xuan, and M. Qi, *Small* **9**, 4237 (2013).

<sup>6</sup>D. M. Tanenbaum, A. Olkhovets, and L. Sekaric, *J. Vac. Sci. Technol. B* **19**, 2829 (2001).

<sup>7</sup>E. J. Boyd and R. J. Blaikie, *Microelectron. Eng.* **83**, 767 (2006).

<sup>8</sup>Y. Matsubara, J. Taniguchi, and I. Miyamoto, *Jpn. J. Appl. Phys.* **45**, 5538 (2006).

<sup>9</sup>J. Kim, D. C. Joy, and S.-Y. Lee, *Microelectron. Eng.* **84**, 2859 (2007).

<sup>10</sup>H. Yang, A. Jin, Q. Luo, J. Li, C. Gu, and Z. Cui, *Microelectron. Eng.* **85**, 814 (2008).

<sup>11</sup>H. Duan, H. Hu, H. Hui, Z. Shen, and J. K. W. Yang, *Nanotechnology* **24**, 185301 (2013).

- <sup>12</sup>B. Cord, C. Dames, J. Aumentado, and K. K. Berggren, *J. Vac. Sci. Technol. B* **24**, 3139 (2006).
- <sup>13</sup>J. K. W. Yang and K. K. Berggren, *J. Vac. Sci. Technol. B* **25**, 2025 (2007).
- <sup>14</sup>J. K. W. Yang, B. Cord, H. Duan, J. Klingfus, S.-W. Nam, K.-B. Kim, M. J. Rooks, and K. K. Berggren, *J. Vac. Sci. Technol. B* **27**, 2622 (2009).
- <sup>15</sup>H. Duan, D. Winston, J. K. W. Yang, B. M. Cord, V. R. Manfrinato, and K. K. Berggren, *J. Vac. Sci. Technol. B* **28**, C6C58 (2010).
- <sup>16</sup>T. Tanaka, M. Morigami, and N. Atoda, *Jpn. J. Appl. Phys., Part 1* **32**, 6059 (1993).

### Figure Captions

Figure 1. SEM image of a 3D supported cross grid structure from sample III fabricated by using the methods described in this paper (tilt angle of 55°). Freestanding top layer was patterned in HSQ and supporting bottom layer was patterned in PMMA. The two layers were exposed in a single electron-beam writing step without intermediate alignment of the pattern.

Figure 2. (Color online) Schematic diagram showing process steps for single-dot exposure process and double-area exposure process. (a) HSQ/PMMA bilayer resist stack was prepared with HSQ on top of PMMA. Both resist layers were exposed from above with an electron beam. The HSQ was overdosed relative to the PMMA, resulting in a larger top structure and overhang. The result was mushroom-shaped posts. (b) The same resist stack as in (a) but the exposure was done by using two immediately sequential doses. In the first lithography step, the bottom layer features were exposed using a high dose, while in the second lithography step, the top layer features were exposed at a dose

that was too low to affect the initial bottom layer exposure. The result was free standing linear HSQ structures supported by PMMA posts.

Figure 3. (Color online) SEM images of 3D nanostructures fabricated from the single-dot exposure process. All structures were from sample II. (a) Mushroom-shaped post structures. (b) Closely spaced linear arrays of posts resulted in connected top layer HSQ patterns supported by PMMA posts in the underlayer. (c) Same post structures as in (a) but where 5.65 times less exposure dose was used. The structures collapsed during the development and drying process.

Figure 4. SEM images of 3D nanostructures fabricated from the double-area exposure process. The first structure was from sample III and the other two structures were from sample I. (a) Mushroom-shaped posts with well-defined top disks over lower posts (tilt angle of  $55^\circ$ ). (b) Freestanding linear top layer structures with a lower layer post support (tilt angle of  $45^\circ$ ). (c) Freestanding cross grid structures with a lower layer post support.